Article:
Dhimish, Mahmoud and Zhao, Xing orcid.org/0000-0003-4000-0446 (2023) Enhancing reliability and lifespan of PEM fuel cells through neural network-based fault detection and classification. International Journal of Hydrogen Energy. pp. 15612-15625. ISSN: 0360-3199

https://doi.org/10.1016/j.ijhydene.2023.01.064

Enhancing Reliability and Lifespan of PEM Fuel Cells Through Neural Network-Based Fault Detection and Classification

Mahmoud Dhimish[1*] and Xing Zhao[1]

[1] School of Physics, Engineering and Technology, Renewable Energy Lab, University of York, York YO10 5DD, UK

[*]Corresponding Author: M Dhimish (Mahmoud.dhimish@york.ac.uk)

Abstract

In order to maximise fuel cell reliability of operation and useful life span, an accurate online health assessment of the fuel cell system is essential. Existing algorithms for fault detection in fuel cell systems are based on sensing elements, control methods, and statistical/probabilistic models. In this paper, an artificial neural network (ANN) will be developed to detect and classify faults in proton-exchange membrane (PEM) fuel cell systems. As the ANN model developed within the PEM system relies on the input and output current and voltage, additional sensing devices are not required within the system. Based on an experimental setup using a 3-kW fuel cell system, it was found that the proposed model was able to detect faults associated with the reduction/increase of fuel pressure, H_2 consumption rate, and voltage regulation changes in the dc-dc converter with >90% accuracy. In the proposed model, historical data is required to train and validate the ANN algorithm, but after this is complete, no human intervention is required afterward.

Keywords: Fuel cell system; Fault detection algorithm; Fault classification; Artificial Neural Networks (ANN); Machine learning algorithm

1. Introduction

Thermal, fluidic, and electrochemical phenomena all play a part in fuel cell energy generation systems. To maintain optimal performance, they need a set of auxiliary elements (valves, compressors, sensors, regulators, etc.) [1]. Because of this, they are susceptible to faults that can lead to fuel cell malfunctions and permanent damage. In addition to heating and cooling systems, humidifiers and cooling systems are also used to ensure that the materials react at optimum conditions [2]. Thermal, fluid-mechanical, and electrolytic phenomena occur during the chemical reaction in the stack, where the energy is generated [3].

In order to implement advanced control techniques and fault diagnosis algorithms based on linear models, the dynamics of fuel cell power generation systems are complex and non-linear. This makes it necessary to use linear models with parameters varying with operating point. Additionally, due to the complexity of such systems' data, some recently developed models for fault identification are based on artificial intelligence (AI) [4,5].

As an example, in a recent study [6], they demonstrated a data-driven fault diagnosis scheme in which the plant model is used only off-line for training the classifier. This paper proposes and tests both support vector machine and random forest classifiers. Using a support vector machine classifier, they found that the data-driven system outperformed the hybrid system in both fault detection and fault identification. This system performs well regardless of how many combinations of working conditions and fault sizes are used.

Fuel cell fault identification is also frequently carried out using heuristic optimization techniques (such as differential evolution, genetic algorithms, and particle swarm optimization [7-10]). Despite the fact that satisfactory results can be obtained based on the fitted model output, the heuristic optimization of non-linear, dynamic models requires considerable computational time and effort. Moreover, an over-parameterized model often results in a non-unique solution to an optimization problem that is ill-posed [11-13]. A false sense of security is created when heuristic optimization techniques are used, suggesting that if a model is highly accurate it must be because the parameters were correctly set.

Considering how highly non-linear the PEM fuel cell model is, it is unreasonable to assume you can use a local linear model to estimate all non-linear parameters [14]. To identify multiple linear structured state space models at once, we must identify multiple linear structured state space models simultaneously [15]. Thus, using AI-based algorithms for fuel cell fault detection is a better option as compared to purely statistical or probabilistic methods. Due to the lack of models and existing techniques for fuel cell AI-based detection systems, further application of AI must be considered as an emerging technology in this research area, which we have attempted to do in this paper.

In essence, AI algorithms are extended subsets of machine learning that teach the computer to operate independently [16]. Through continuous learning, the device improves processes and runs tasks more efficiently as a result. There are three types of machine learning algorithms: unsupervised, semi-supervised, and reinforcement learning. Classification, regression, and forecasting fall under supervised learning [17-20], while semi-supervised learning uses both labelled and unlabelled data [21]. The difference between labelled and unlabelled data is that labelled data has meaningful tags for the algorithm to understand, while unlabelled data lacks those tags.

An algorithm used in reinforcement learning receives a set of actions, parameters, and end values to determine how to proceed [22,23]. In order to determine which option is the best, the machine learning algorithm explores different options and possibilities, monitoring and evaluating each result as it goes along. The machine learns by trial and error through reinforcement learning. In response to the situation, it adapts its approach based on past experiences to achieve the best results.

There are several factors to consider when choosing an algorithm for machine learning, such as the size, quality, and diversity of the data, as well as the answers businesses want to obtain from the data. There are many other considerations as well, including accuracy, training time, parameters, and data points. For example, an artificial neural network (ANN) [24-26] is built up of a series of layers, each with a connection to the layer adjacent to it. Brains and other biological systems are used as models for ANNs. This ANN is made up of many interconnected processing elements that are integrated to solve specific problems. One example is solving the nonlinear characteristics of the dataset of full cell systems by focusing on the high degree of detail in the points. Therefore, in our work we have carefully considered the advantages and disadvantages of ANN over other AI-based techniques. The purpose of this is to ensure the success of the real-time fault detection algorithm when applied to a fuel cell experiment setup.

This paper presents ground-breaking work on developing a highly accurate ANN-based model for fuel system fault detection. Our model considers six different types of faults, including fuel pressure, H_2 consumption rate, and dc-dc converter regulation faults, and is validated using a variety of experimental tests based on real-time measurements from a fuel cell system. The results show that our model is capable of detecting fuel cell system faults with an impressive accuracy rate of over 93% in most cases. This work has significant implications for the field of fuel cell technology and represents a significant advancement in the field.

The paper is organized as follows: Section 2 presents the methodology including fuel system setup, fault types, and ANN model. In section 3, we present the results of our proposed fault detection model and compare it to other recently published papers. Lastly, section 4 concludes the work and proposes future directions.

2. Methodology

2.1 Fuel system and dc-dc converter Setup

In this study, an ANN evaluation is used to evaluate a 3.0 kW hydrogen PEM fuel cell system. For the fuel cell to produce its peak output power, it requires pure hydrogen gas (0.99%) at 0.5 bar pressure. Compressed hydrogen gas at 175 bars provides the low-pressure hydrogen supply. Overpressure safety vents and purge/drain points are installed as well as the controls.

An output voltage range of 50 V to 105 V is provided by the fuel system. The output terminals are connected to a buck/boost dc-dc converter with an efficiency of 98.5%. To utilize this converter with purely resistive loads, the output terminals are connected to the converter. Figures 1(a-d) shows the fuel cell, ventilation system, test chamber for a fuel cell, and the detailed schematic of the fuel cell system.

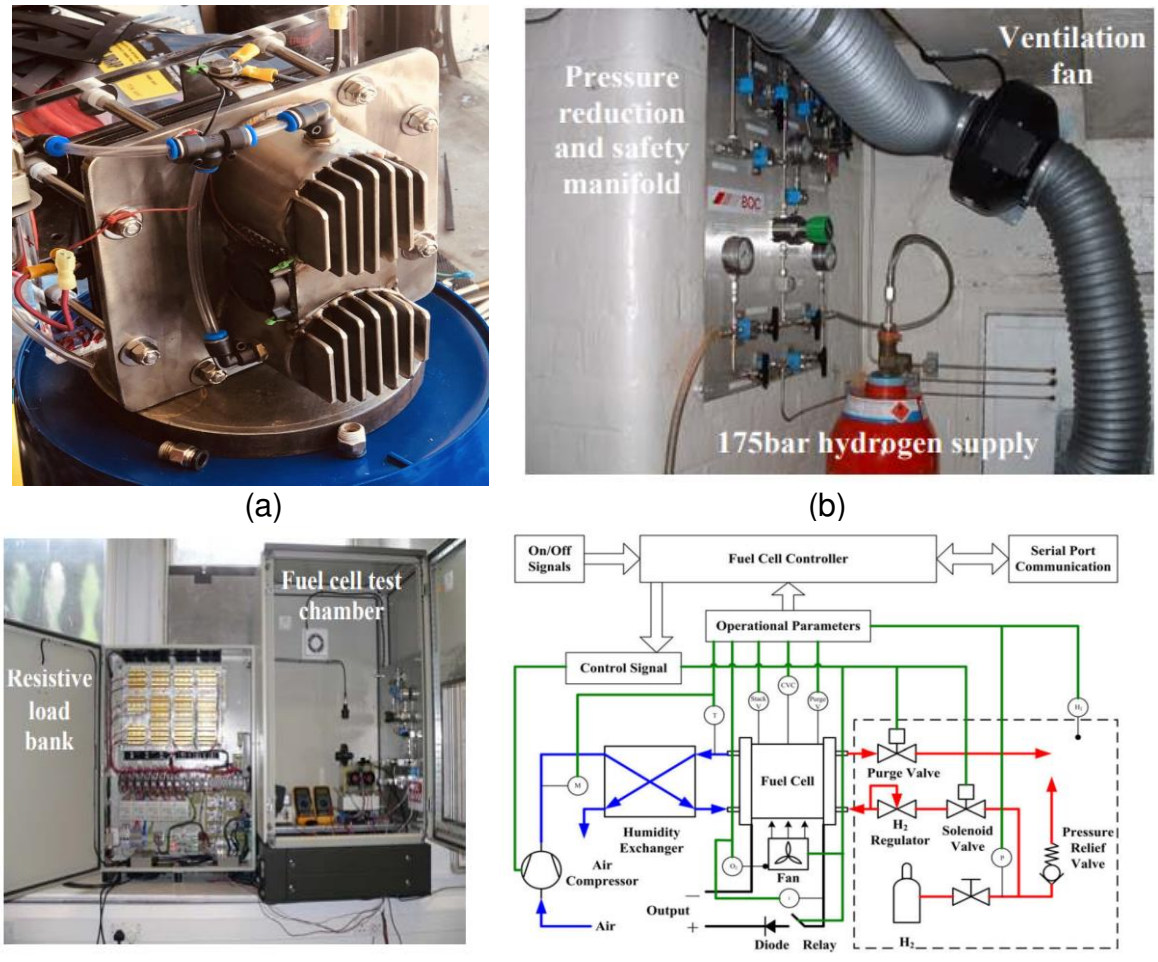

(a) (b)

(c) (d)

Figure. 1 – (a) Fuel cell setup, (b) Fuel cell hydrogen supply, (c) Resistive load and the fuel cell chamber, (d) Detailed schematic of the fuel cell system.

In Figure 2, the output characteristics of a fuel cell system (voltage versus current) at varying pressure are shown. It can be noted that as we increase the fuel pressure, we are expected to see an increase in the output voltage

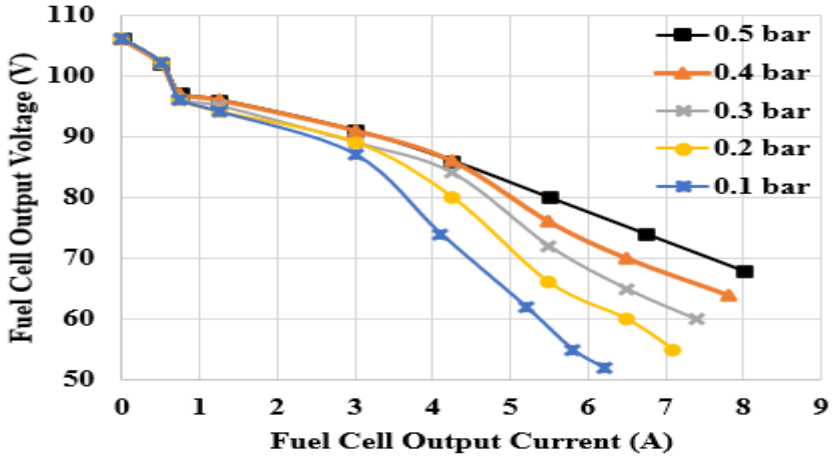

Figure. 2 – Voltage-current curve characteristics of the fuel system at varying fuel pressure.

The key characteristics of the fuel cell and the dc-dc converter are summarized in Table 1. Fuel cell systems consume 39 L/min of H_2 at full load, and the maximum stack temperature should not exceed 69°C. By feeding the converter's main input terminals with fuel cell power, the fuel cell system can achieve a continuous working cycle.

Table 1 – Fuel cell and dc-dc converter key characteristics

Parameter	Value (unit)
Fuel cell system	
Unregulated output voltage range	50 – 105 Vdc
H_2 consumption at full load	39 L/min (0.2 Kg/h)
Maximum rated output power	3 kW
Total Number of cells	120 (2 x 60 per stack)
Maximum Stack temperature	69 °C
Fuel supply	Pure hydrogen (0.99)
Working cycle	Continuous
dc-dc converter	
Converter power rating	3.5 kW
Input voltage range	40 – 175 V
Output voltage range	24 – 48 V (buck); 72 – 96 (boost)
Input maximum current	20 A
Conversation efficiency	99% at full load

Increasing fuel pressure increases the output power of the fuel cell system (Figure 3). The maximum power obtained when purging the system with fuel pressure of 0.5 bar, for example, was 2835 W. On the other hand, the maximum power at 0.1 bar is 2135 W.

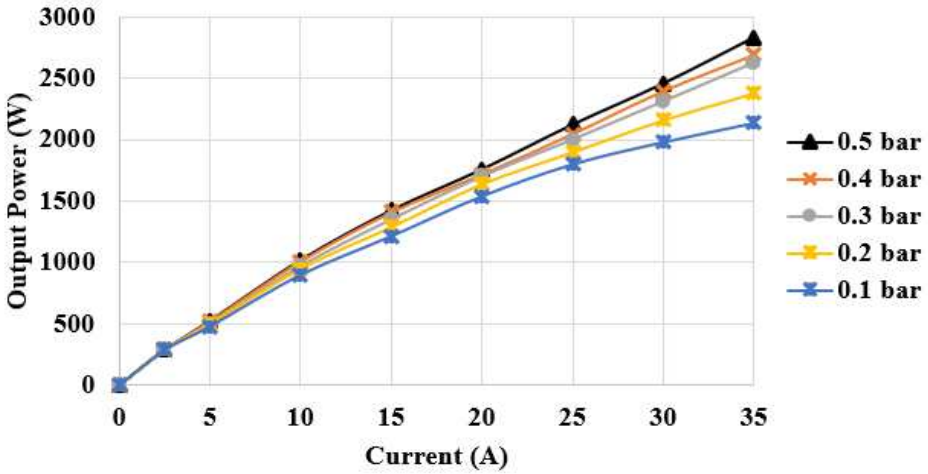

Figure. 3 – Power-current curve characteristics of the fuel system at varying fuel pressure.

As a test to determine whether the dc-dc converter has a stable output voltage, the converter was tested at a fixed output voltage of 36 V while varying the fuel pressure. Based on the results shown in Figure 4, the maximum ripple (variation of converter output voltage) is 0.12 V, proving the precision of high voltage conversions. In this case, we can also see that the converter can observe the fluctuations in the fuel cell input voltage and mitigate them accurately.

Tests such as these were conducted to confirm the quality of the converter, which could then affect the accuracy of the ANN algorithm. A converter, for example, may have a wide range of voltage ripples, which must be implemented or compensated later in the development of the ANN network. However, Figure 4 explains that the converter's regulated voltage varies only slightly.

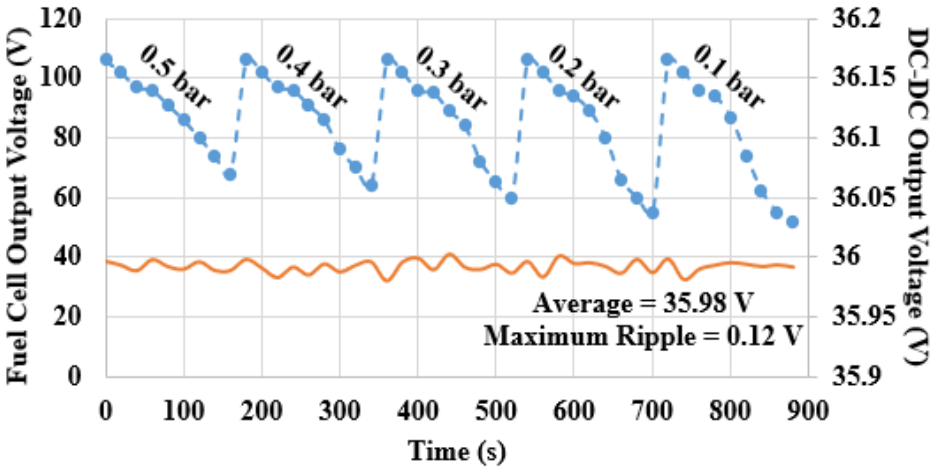

Figure. 4 – Output voltage of the dc-dc converter at varying the fuel cell voltage.

2.2 Fault types

It is possible for the fuel cell system, including the converter, to suffer from various types of faults. It is relatively easy to distinguish faults such as drying, or flooding since they require monitoring the water level in the system. In addition, the hydraulic faults such as the decrease in compressibility or the mechanical fault such as crank shaft stall can also be monitored by checking the friction rate of the fuel cell, as well as the controller's fault, which is easily detected (when the controller breakdowns or the monitoring unit lags). Our work focuses on the detection and classification of six fault categories that are hard to detect by observing only parameters of the entire system; they are presented in Table 2. One reason is that these fault categories may not be directly reflected in the parameters of the entire fuel cell system. For example, if a fault is occurring within a specific component of the fuel cell system, it may not be immediately apparent by looking at the overall performance or output of the system. Another reason is that the fault categories considered in this work are difficult to distinguish from other types of faults or normal variations in the system. For example, if the system suffers from low/high voltage regulation of the dc-dc converter which might end up causing a small change in the fuel cell system's performance, it may be difficult to detect this change among the normal variations that occur within the system. Overall, the complexity of fuel cell systems and the various factors that can affect their performance make it challenging to accurately detect certain types of faults by observing only the parameters of the entire system, and hence, the development of an AI-based system is a suitable solution to solve such challenge.

Table 2 – Fuel cell fault categories considered in this work

Class number	Fault Type
Class 1	Normal operation mode
Class 2	Reduction in the fuel pressure
Class 3	Increase in the fuel pressure
Class 4	Reduction in the H_2 consumption rate
Class 5	Increase in the H_2 consumption rate
Class 6	High voltage regulation of the dc-dc converter
Class 7	low voltage regulation of the dc-dc converter

In anticipation of developing an intelligent tool to detect these faults, the first class was introduced to ensure that there is a category without faults. Classes 2 and 3 indicate whether the fuel system has the correct level of fuel pressure. We have seen in Figure 3 that if the system is not supplied with enough pressure, its output power will drastically decrease. Contrary to this, classes 4 and 5 indicate H_2 consumption levels. With increasing output system current, the consumption rate is expected to increase. The low/high rate indicates a problem with the fuel level, so it is usually a sign of low/high fuel.

In the last classes, we will detect whether the converter's regulation is higher or lower than expected. The output converter's voltage might go down from 24 V to 12 V and still be connected to the load without any fault identification even though it can be monitored externally (with a voltmeter). The problem usually occurs when the converter's current rating is restricted, so the voltage is reduced (buck) to a lower value.

The outputs of the fuel cell system parameters (voltage and current) and the converter outputs (voltage and current) can be used to observe changes in these different faults, as shown in Figure 5. The output measurements are then logged into a database (Google cloud) and processed using MATLAB software to develop an ANN model. As a consequence, the ANN algorithm is able to first indicate the fault and then to classify it according to the classes mentioned above (class 1 to 7). The architecture of the proposed ANN model will be discussed in more detail in the next section.

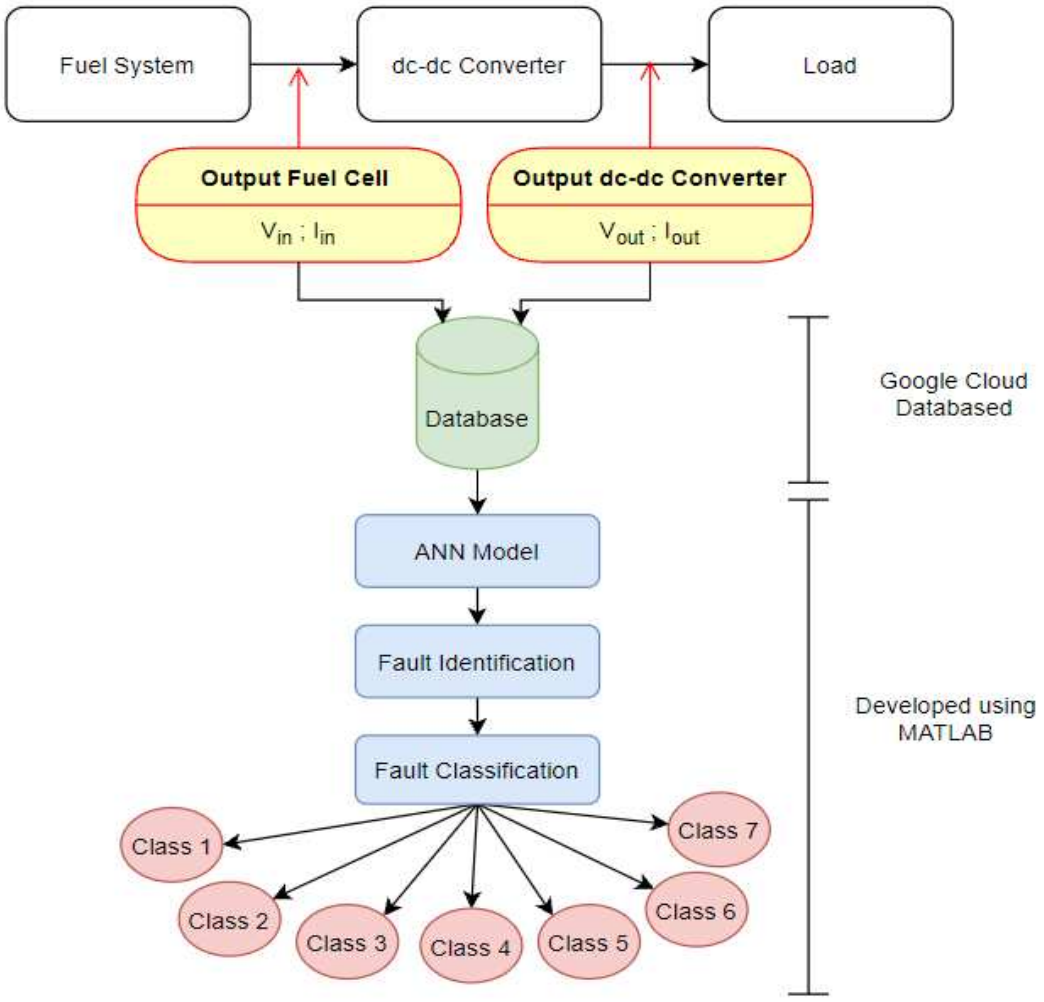

Figure. 5 – Flowchart of the developed algorithm.

2.3 Proposed ANN model

Four inputs are used to implement the ANN (fuel cell output voltage and current and converter output voltage and current). A hidden layer containing eight neurons is formed from these inputs. An extensive simulation process was used to determine the number of neurons. Thus, the MATLAB program ran from 1 to 100 neurons. A maximum ANN training accuracy of 98.6% was achieved at eight neurons, as shown in Figure 6.

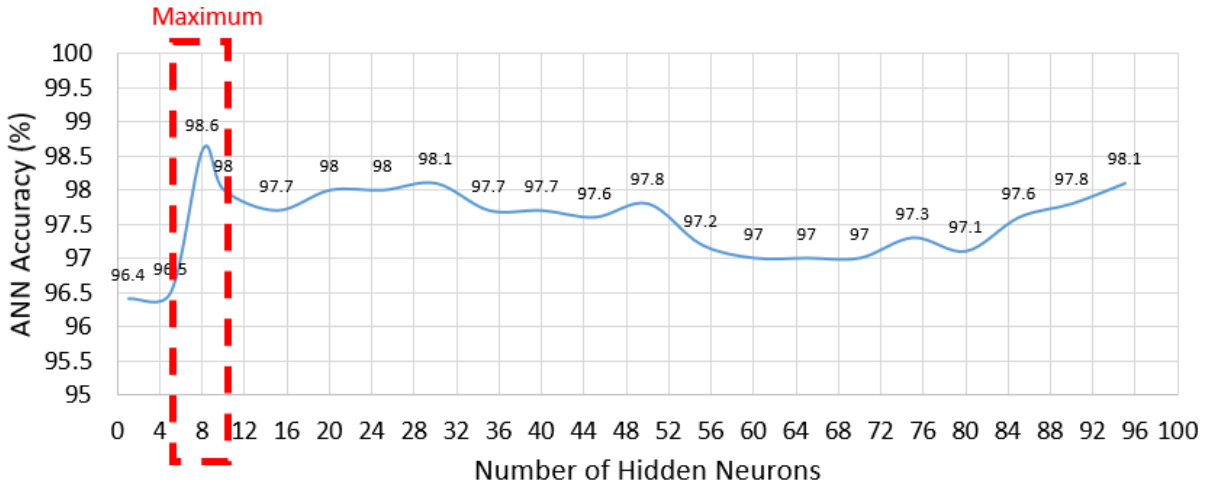

Figure. 6 – Number of hidden neurons vs ANN accuracy.

Each neuron in the hidden layer takes a formed linear combination of the outputs of previous neurons. This linear combination is weighted using the strength between the neurons (w_{ij}) and multiplied by both inputs (x_j). An activation threshold (w_{j0}) was also assigned to each neuron. This process is expressed using (1). Note: *i* is equal to number of hidden neurons (1 to 8), *j* is equal to number of inputs (1 to 4).

$$\sum_{j=1}^{4}(w_{ij}x_j + w_{j0}) \quad (1)$$

The weighted activation process is then multiplied by the non-liner function f_1 as shown in (3), this is done using a sigmoid function, $f_1 = \frac{1}{1+e^{-x}}$. Finally, the output value of the hidden layers y_i is determined by (3).

$$f_1 \times \sum_{j=1}^{4}(w_{ij}x_j + w_{j0}) \quad (2)$$

$$y_i = f(u) = \frac{1}{1+ e^{-\sum_{j=1}^{4}(w_{ij}x_j + w_{j0})}} \quad (3)$$

There are seven different classes in the output layer, each representing a specific condition (these classes have already been discussed in the previous section). The overall architecture of the developed ANN model can be seen in Figure 7.

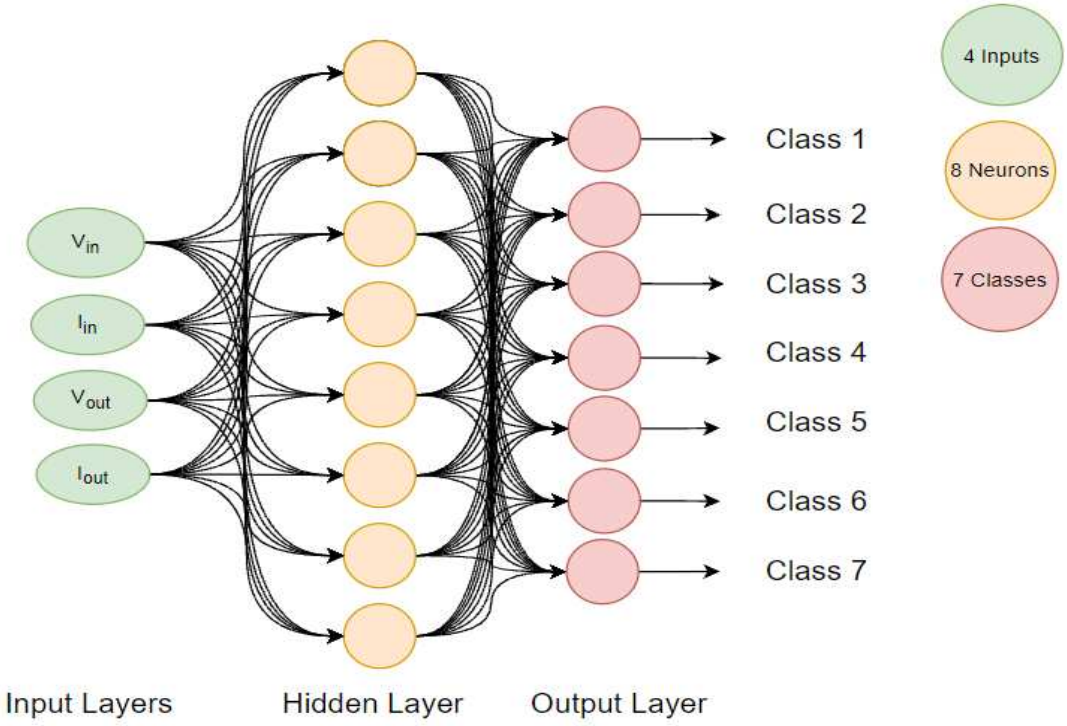

Figure. 7 – Developed ANN model architecture.

A summary of the ANN model characteristics is presented in Table 3. The model comprises four inputs and a single output using one hidden layer. The training process is supervised, meaning that we provided a set of input/output data of appropriate network behaviour. We randomly divided 85% of the samples for training, 15% for validation. The training algorithm chosen is Levenberg-Marquardt, considering it is a faster algorithm for networks of moderate sizes. The data were randomly selected for training and validating, and all data samples were normalised to 0 to 1 range using (4). Here $i \in \{i_{min}, i_{max}\}$ is the original data value, and $J \in \{j_{min}, j_{max}\}$ is the corresponding normalised value with $j_{min} = 0$ and $j_{max} = +1$.

$$J = \frac{(j_{max} - j_{min})(i - i_{min})}{(i_{max} - i_{min})} + j_{min} \quad (4)$$

In order to prevent overfitting of the ANN model, the dropout rate is used. Input and hidden layers dropout at a rate of 0.5. Weights are set to zero to initiate the dropout process. There are 100 iterations in the training process, and there are 10 batches.

The Levenberg-Marquardt algorithm is an optimization algorithm that is often used in training ANNs. It is a hybrid algorithm that combines the features of both gradient descent and the Gauss-Newton algorithm, and it is known for being efficient and effective at minimizing the error between the predicted outputs of the ANN and the target outputs. In the training process, the Levenberg-Marquardt algorithm works by iteratively adjusting the weights and biases of the ANN to minimize the error between the predicted and target outputs. It does this by calculating the gradient of the error function with respect to the weights and biases and using this gradient to update the weights and biases in a direction that reduces the error. The algorithm also utilizes a damping factor to balance the importance of the gradient descent and Gauss-Newton steps, and to prevent the algorithm from oscillating or diverging.

We have considered using Sigmoid activation function, defined in (5), where x is the input to the function and e is the base of the natural logarithm. Below are the Sigmoid key characteristics that contributed to the choice for its use in our work:

- It maps the input values to a range of 0 to 1.
- It is continuously differentiable, which makes it suitable for use in backpropagation algorithms for training ANNs.
- It has a smooth and monotonic shape, which allows it to approximate a wide range of functions.
- It saturates at the extremes of the range, which can cause problems with the training process if the inputs to the function are not properly scaled.

$$f_{(x)} = \frac{1}{1+e^{-x}} \tag{5}$$

Table 3 – ANN model characteristics

Parameter	Value
Input variables	4 (V_{in}, I_{in}, V_{out}, I_{out})
Output variables	7
Number of hidden layers	1
Number of neurons	8
Training process	Supervised
Training algorithm	Levenberg-Marquardt
Activation function	Sigmoid
Type of division samples	Random
Training	85%
Validation	15%
Normalization	(0,1)
Dropout rate for input layer	0.5
Dropout rate for hidden layer	0.5

Real-time data measurements were used to train the ANN model. Figure 8(a) shows the fuel cell system voltage and output power at different pressures (0.1 to 0.5 bar) and loading conditions (full and half-load). Additionally, Figure 8(b) shows H_2 consumption rates during the experiment.

A sampling rate of one sample per second was used in this experiment, with the pressure remaining at the same level every five minutes. A total of 3000 samples were collected for each parameter. Later in the next section, we will demonstrate that the ANN network was not overtrained.

In this case, it is reasonable to observe changes in the fuel cell system output voltage and H_2 consumption rate at full-load (at 35 A). By contrast, we are unlikely to observe a difference in measurements as the load decreases (at 15 A). Even though the fuel pressure changed, there were no noticeable differences in H_2 consumption rate. As a result, this is another compelling reason why ANNs are appropriate for solving such problems. Contrary to the data, the model can detect minor changes, and the variations of all parameters are classified accordingly.

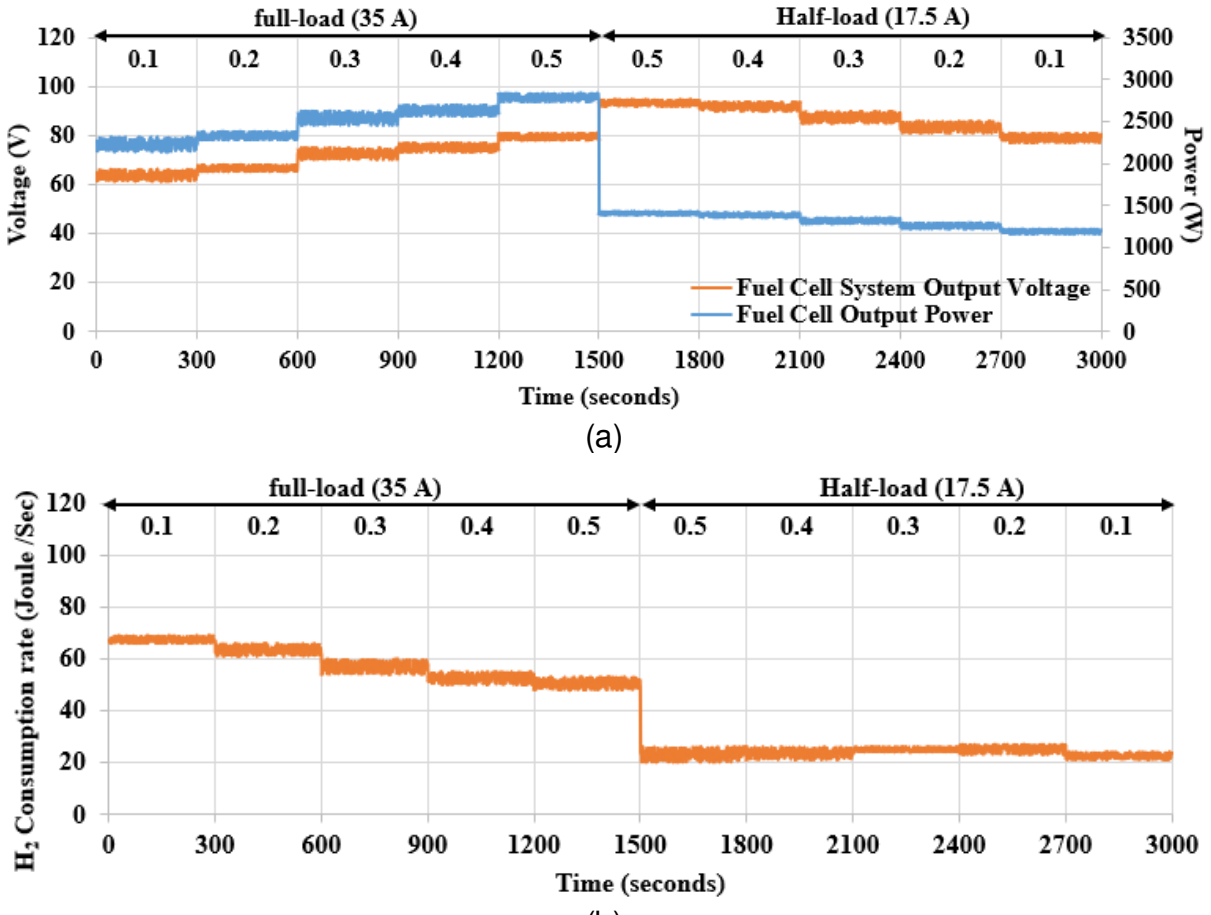

Figure. 8 – Output measured data. (a) Fuel cell system voltage and power, (b) H_2 consumption rate.

According to Figure 8(a), the output voltage of the converter was 36 V at the beginning of the experiment, but 48 V when the half-load was applied. In addition to measuring the output power at load, Figure 9(b) illustrates the converter's efficiency (always greater than 97.5%). In order to calculate the efficiency, we used (6). Furthermore, Figure 9(c) shows a 98.7% fit curve between fuel cell system power and dc-dc converter power.

$$Efficiency = \frac{Output\ Power\ at\ Load}{Otput\ Power\ of\ the\ Fuel\ Cell\ System} \times 100\% \quad (6)$$

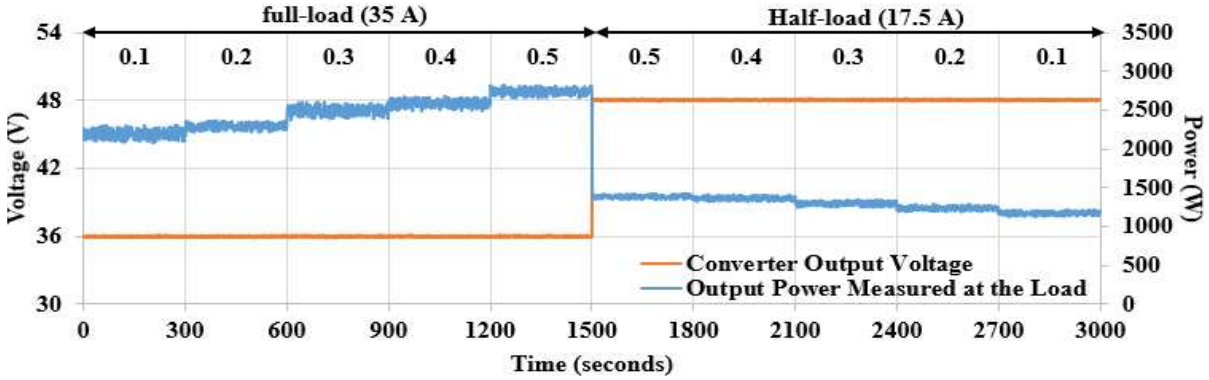

(a)

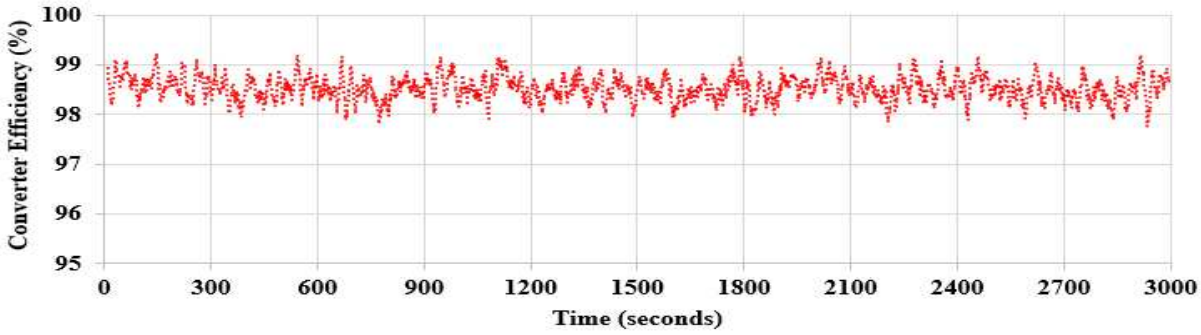

(b)

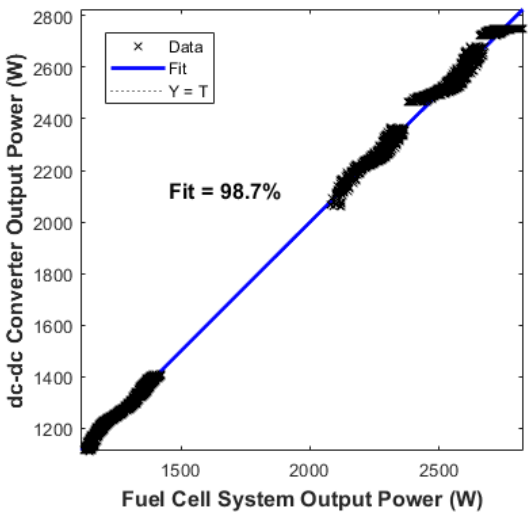

(c)

Figure. 9 – (a) Output measured data of the dc-dc converter voltage and power at the load, (b) Converter efficiency, (c) Fit curve for the output power.

An ANN model was trained using the data set shown in Figures 8 and 9. 85% of the data were used for training, and 15% for validation. As this will be evaluated using a different data set (discussed in the next section), we did not choose any data for testing. This confusion matrix shows the model's training and validation confusion, where red labels indicate classes that have been misclassified and green diagonal labels indicate samples that have been correctly classified. Achieving accuracy rates of 99.3% and 98.6% for training and validation, respectively, suggests that the model is able to accurately classify the different fault categories in most cases.

Figure 10(b) shows the cross-entropy versus epochs to ensure no overtraining hinders the proposed model. We can note that the ANN model needs to be reprocessed 32 times (32 epochs) to achieve a cross-entropy of 1.63% for its best validation. In this case, we can conclude that there hasn't been any overtraining in the network as a result of the low cross-entropy rate. According to Figure 10(b), the training and validation are almost saturated.

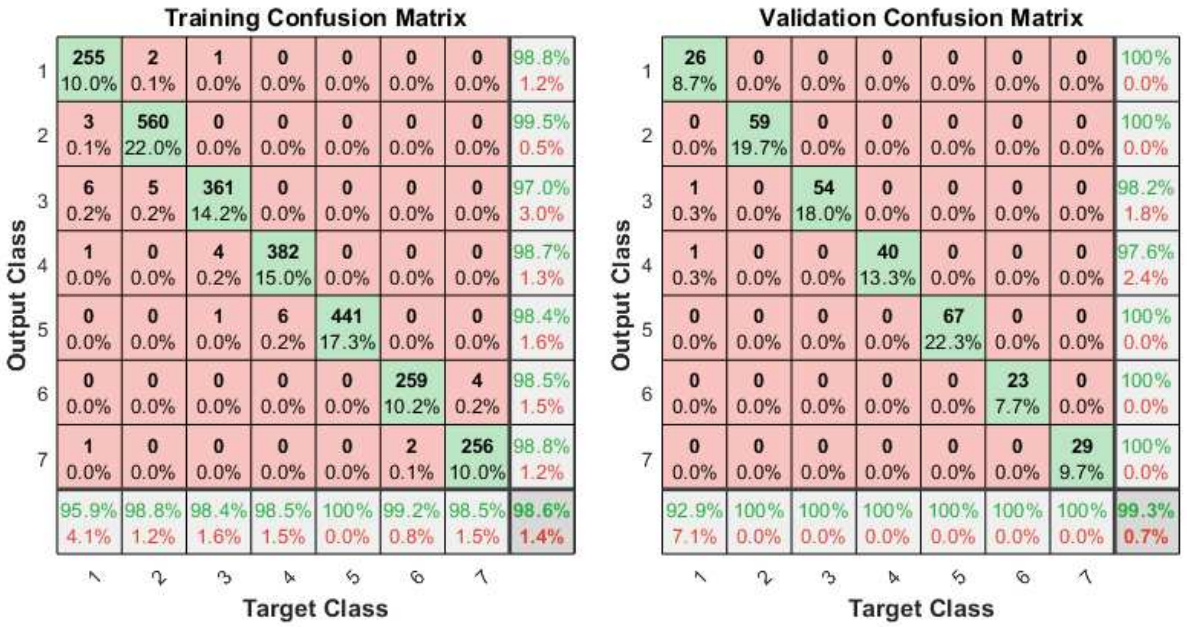

(a)

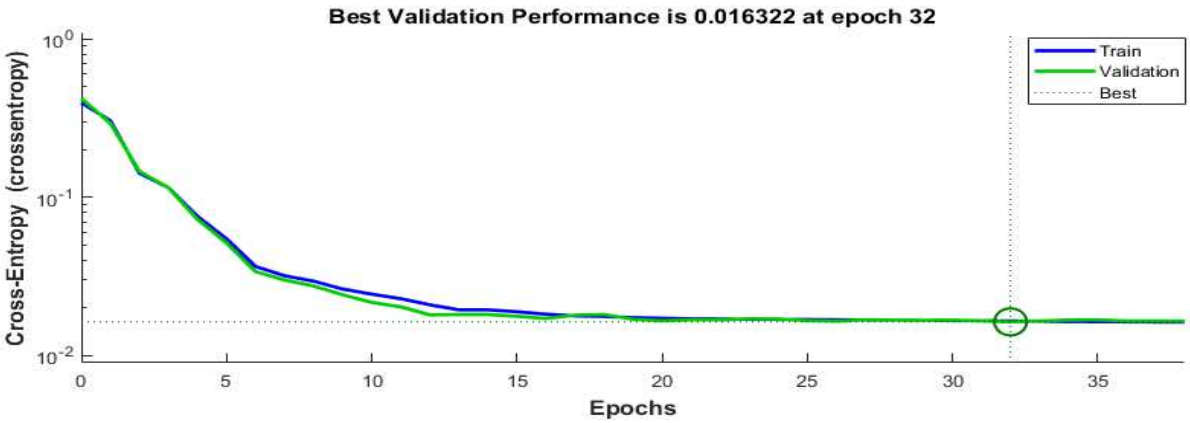

(b)

Figure. 10 – (a) ANN training and validation confusion matrix, (b) Best validation performance.

A receiver operating characteristic curve (ROC) shows the performance of ANN models at all classification thresholds. In the end, it shows a correlative relationship between the true-positive and false-positive rates of the different classes. Detecting the correct class classification is more likely when the true positive is higher (ideally 1 = 100%).

According to Figure 11, the ROC response for the developed ANN model is displayed for all classes during training and validation. A true positive rate of 0.99 was observed for all classes. A ROC of 0.96 was observed for class 1 as the lowest.

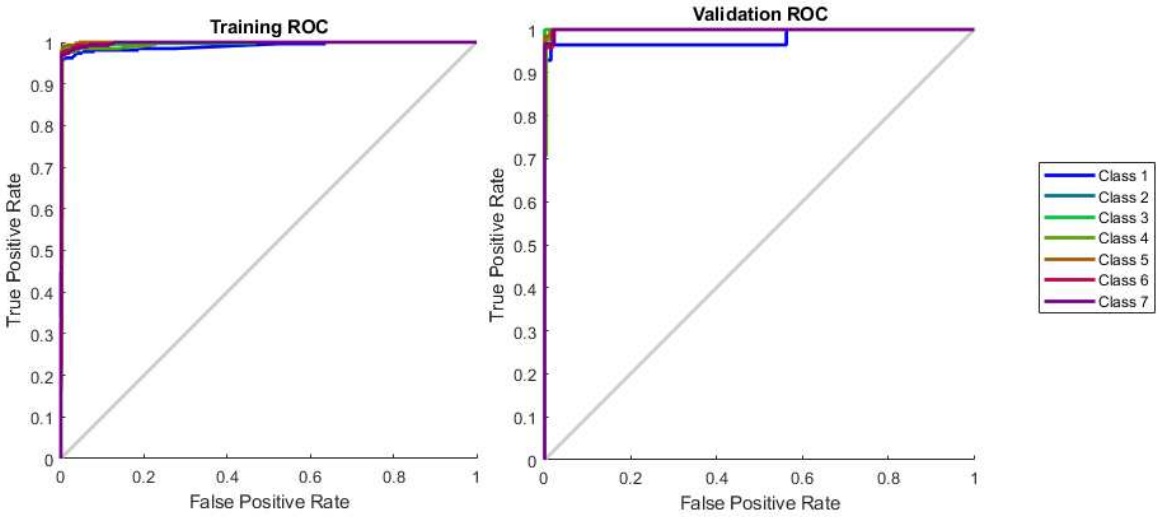

Figure. 11 – ROC response of the developed ANN network.

3. Results

3.1 Test #1

A total of 300 samples were collected by different experimental routines, each lasting 5 minutes at a sampling rate of 1 sample/second. Figure 12 shows the measurements of the fuel cell system and the dc-dc converter. As a matter of fact, the data records in Figure 12 are the input data for the ANN model that predicts the output operating class (faulty condition). Accordingly, the system's normal operating condition (class 1) is used when the fuel pressure is 0.4 bar and the dc-dc converter is set at 36 V (as shown by the first 300 samples). As a result of the second cycle, the fuel pressure has decreased to 0.3 bar, while in the subsequent cycle, the fuel pressure returns to its normal level.

Fuel pressure increased after 15 minutes (900 seconds) (fault class category 3). The system was reset to normal operation in the 1200s - 1500s. From 1500 to 1800, the voltage regulation of the dc-dc converter was increased to 48 V (class 6), while between 1800 and 2100, it was reduced to 24 V (class 7). From 2100s onwards, the system is operating normally.

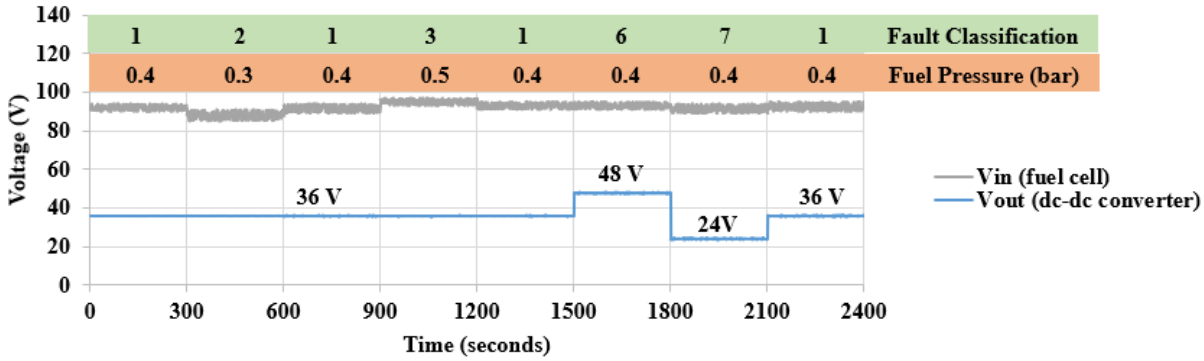

(a)

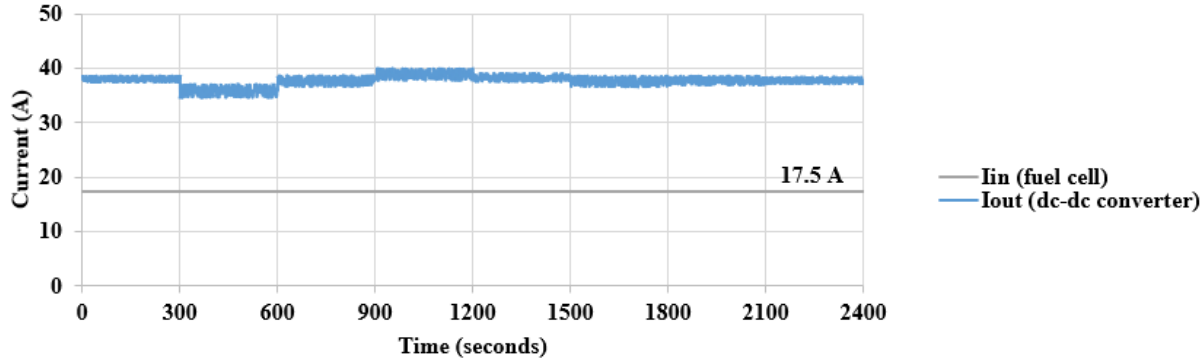

(b)

Figure. 12 – Test #1. (a) Voltage measurements, (b) Current measurements.

Based on the data from this experiment, Figure 13(a) shows the accuracy of predicting the correct class (fault condition). Three key findings are expressed in the confusion matrix,

1) The ANN model predicted the various fault conditions applied to the fuel system and dc-dc converter with an accuracy of 93.4%.
2) Due to the fact that we have not taken the rate of H_2 consumption into account, the ANN model accurately did not include any samples within these two classes (see row of output class 4 and 5, no samples are observed).
3) The most misclassified data (93 samples) were obtained when the system was operating normally. Due to rapid fluctuations in the faulty routines during the experiment, this is expected. By contrast, it is impressive to confirm that 93% of the changes in voltage levels for dc-dc converter can be predicted based on the ANN model as shown by output classes 6 and 7.

In Figure 13(b), the ROC response of the ANN model shows that class 2 had the lowest true-positive rate of just over 0.9. This is due to the fact that the output voltage of the fuel cell system drops insignificantly when the fuel pressure is reduced (class 2). Therefore, predicting the fault condition with just a few data samples (in our case, 300 samples were used) can be quite challenging. Despite this, a true-positive rate of 90% resembles excellent performance. For all other classes, however, the true-positive rate is always above 0.95.

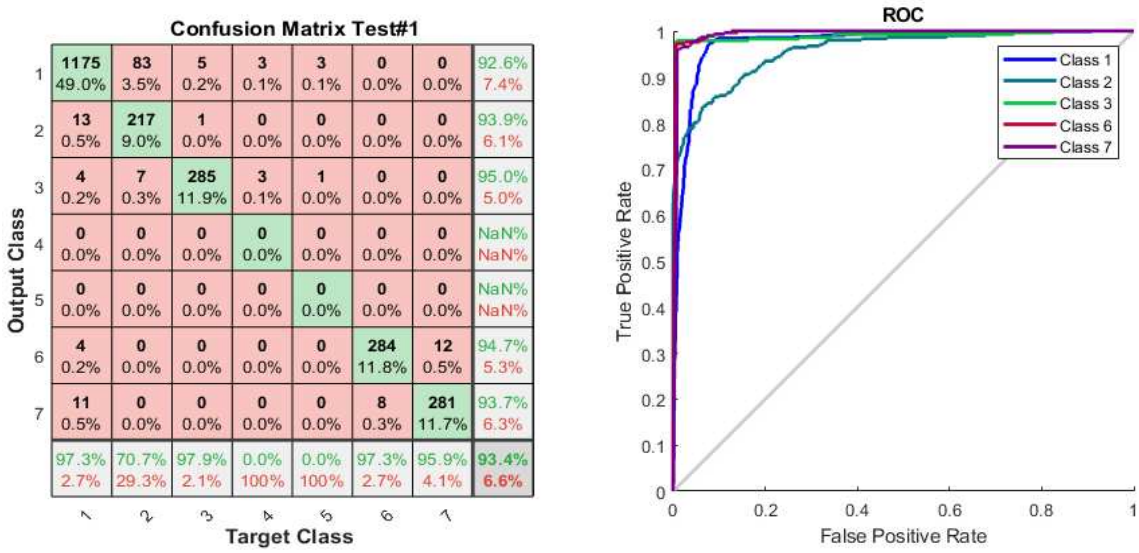

(a) (b)

Figure. 13 – Output results of the ANN model using the data measurements of test#1. (a) output confusion matrix, (b) ROC response.

3.2 Test #2

During this test, different routines were applied to the fuel cell system. Figure 14 shows that each experiment lasted for 5 minutes with a sampling rate of 1 sample/second, totalling 300 samples/routine. Like the previous section, the system's normal operating condition (class 1) is achieved when the fuel pressure is 0.4 bar, and the dc-dc converter is set to 36 V (presented by the first 300 samples). Using the second routine, the level of H_2 in the tank is increased in an attempt to reduce H_2 consumption. As a result of the same reduction in H2 level in the third cycle, the converters' voltage is also decreased to 24 volts.

During the fourth cycle, the H_2 in the tank is increased to achieve Class 5. During the sixth cycle, however, the H_2 level is maintained and the output voltage of the converter is changed to 48 volts, restoring the system to its normal state.

Finally, the system was operating under two faulty conditions during the 1800s-2100s, a reduction in fuel pressure (0.3 bar) and a reduction in H_2 consumption. This system was operated under an increased fuel pressure (0.5 bar) in the last cycle, as well as a higher H_2 consumption rate.

Figure 15 shows the confusion matrix of the ANN model using the data of this experiment. Overall, 94.5% of the faulty conditions were detected accurately. Class 4 and 5 achieved 89.8% and 91.4% detection accuracy, respectively, while classes 6 and 7 achieved 100% detection accuracy. The ROC response, Figure 15(b), confirms the same conclusion since class 4 and 5 true positive rates are nearly 0.9, compared to roughly 0.99 for all other classes.

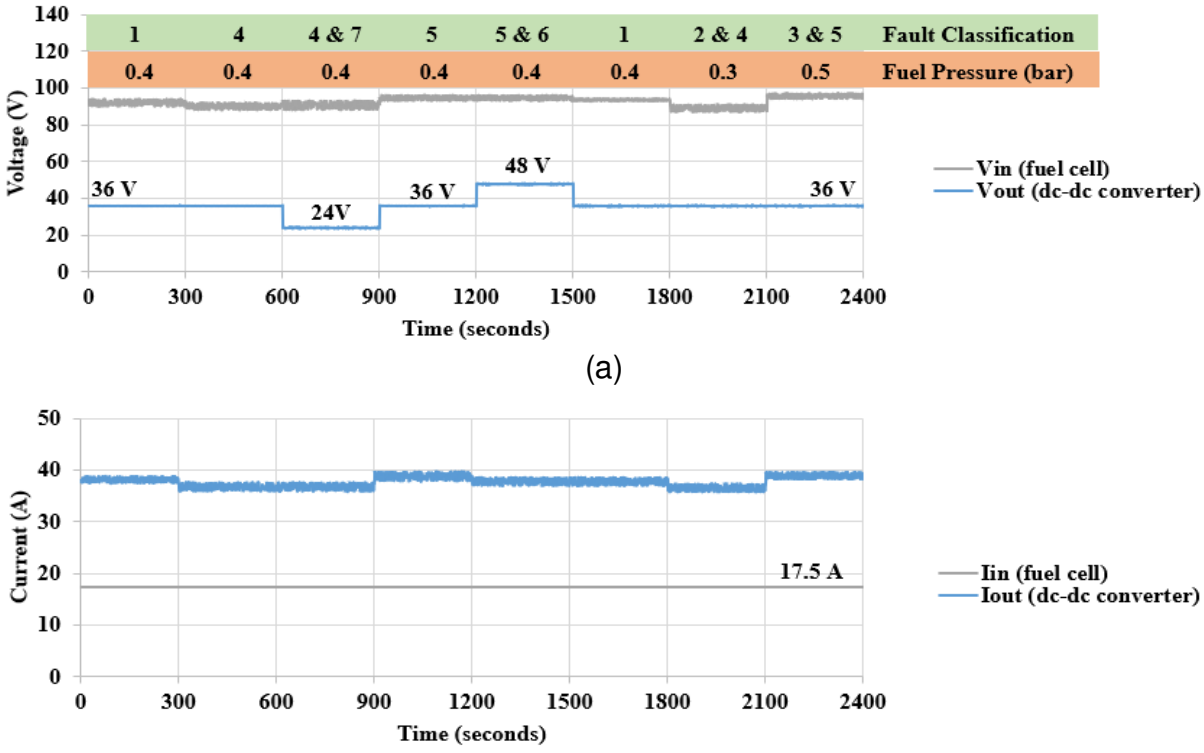

Figure. 14 – Test #2. (a) Voltage measurements, (b) Current measurements.

The data for Classes 4 and 5 are more difficult to classify or distinguish from other classes. This is due to a number of factors, such as the similarity of the data to other classes, the presence of noise or other confounding factors, and the complexity of the relationships between inputs and outputs. In addition, changes in the H_2 consumption rate may be small or subtle, making it difficult to detect them by observing only the parameters of the entire fuel cell system. In addition, the H_2 consumption rate may be influenced by a variety of factors, such as the load on the fuel cell, the temperature and humidity of the environment, and the age and condition of the system. These factors can make it challenging to accurately attribute changes in the H_2 consumption rate to specific faults.

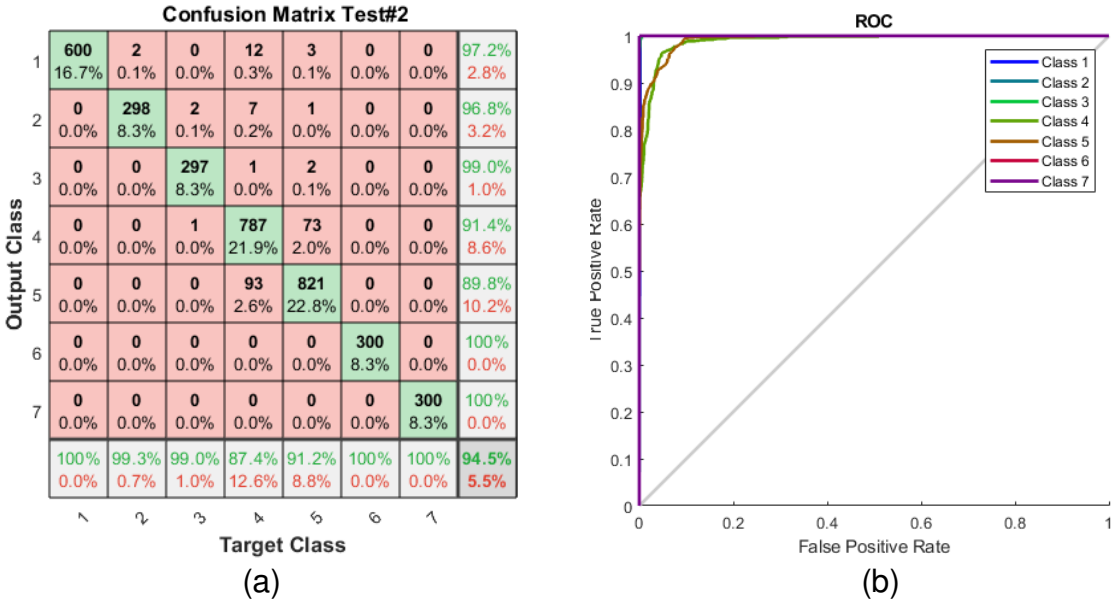

Figure. 15 – Output results of the ANN model using the data measurements of test#2. (a) output confusion matrix, (b) ROC response.

3.3 Comparative Study

In Table 4, we compare the proposed work to several relevant papers [27-31] on fuel cell fault diagnostics. One key difference is that we propose identifying failure modes such as changes in H_2 consumption rate or dc-dc converter regulation, which have not been addressed in previous work. While data-driven fault diagnostic methods have been used in [27-29] to identify flooding issues in fuel cell systems, these tasks are relatively straightforward due to the availability of modern sensing devices. In contrast, our work defines seven different types of operational conditions and uses an ANN-based approach to detect faults. In [31], an ANN-based method is also used for fuel cell fault detection, but without categorizing the faults. Additionally, [30] proposes using BinE-CNN to detect faults based on images of the fuel cell system. However, this approach requires the input of images and may not function without them.

Table 4 – Comparison of this work with recent work in fuel cell fault identification [27-31]

Ref	Year	Technique	Fuel Cell System Fault Types	Average Detection Accuracy
[27]	2019	In this diagnostic approach, advanced features are extracted and patterns are classified based on the individual fuel cell voltage signal and an algorithm is developed to accomplish this	High air stoichiometry, flooding, membrane drying, and high stack currents or temperatures	85% to 94%
[28]	2020	Fuel cell powered systems are designed with diagnostic algorithms that use lumped modelling as a method of fault mitigation based on model-based mathematical methodology	A generic method of identifying fault signals received by a fuel cell system. There has been no discussion of specific fault categories	82% to 96%
[29]	2021	Based on the embedded platform, a Long Short-Term Memory (LSTM) network model is developed and applied to flooding fuel cell system fault diagnosis.	Flooding	Not mentioned
[30]	2022	Using binary matrix encoding neural networks, a fault diagnosis algorithm called BinE-CNN is proposed. BinE-CNN achieves seven-category fault classification through the extraction of high-dimensional features using binary encoding and convolutional neural networks (CNNs)	Slight or sever drying, slight or severe flooding, and slight or severe starvation of the fuel cell system	Experimentally 95.1% Simulation 97%
[31]	2022	Data-driven approach using ANN and sensor pre-selection. For sensitivity analysis, time-domain and frequency-domain features of sensor data are extracted.	There is no categorization of the fault. By using the model, you can determine whether or not the fuel cell system has encountered a fault	99.2% but only to indicate if the fuel cell is faulty
This work	2022	ANN model developed within the PEM system relies on the input and output current and voltage, additional sensing devices are not required within the system.	Increase/decrease in the fuel pressure, increase/decrease in the H_2 consumption rate, and DC/DC converter regulation	90% to 95%

4. Conclusions

ANN-based model is proposed in this paper for the detection of faults in PEM fuel cell systems. A seven-type fault system is developed, which takes fuel pressure, H_2 consumption rate, and DC/DC converter regulation into account. As a starting point, the ANN network was trained using measurements taken from a laboratory experiment using a 3-kW fuel cell system operating at various pressures (0.1 to 0.5 bar). In summary, the results of the ANN are as follows:

1) Greater than 95% accuracy is always achieved in detecting increases or decreases in fuel pressure.
2) Any change in the dc-dc converter regulation voltage can be detected with an accuracy rate of at least 93%.
3) When the H_2 consumption rate is reduced or increased in the fuel cell system, the ANN model has the lowest detection accuracy of about 90%. During this particular operational condition, the parameters of the fuel cell system do not change significantly, so it is likely that the ANN will misclassify the fault type.

In this work, the ANN model is trained on inputs and outputs of current and voltage from PEM fuel cell system. Thus, if the fuel cell system does not have monitoring units or sensing elements, our proposed model is unlikely to be as effective as it can be when such parameters are present. While datasets are initially required to run our proposed model, it can be run without human intervention, making it easier to run the algorithm and detect the full cell system fault without any additional input requirements.

There are a few possible ways to extend this work on detecting and classifying faults in fuel cell systems using artificial neural networks (ANNs). One potential direction is to develop a more generic AI model that can be applied to fuel cells of different capacities and types. This could involve training the model on a diverse dataset of fuel cell systems in order to improve its generalizability and adaptability to different environments and operating conditions. Another possibility is to incorporate a fuzzy logic sub-layer into the neural network model to improve the accuracy of fault classification and mitigate misclassified fault categories. Fuzzy logic can be used to represent uncertainty and imprecision in the data, allowing the model to make more nuanced and context-dependent decisions. This could be particularly useful for handling complex and subtle fault patterns that may be difficult to identify using traditional statistical or probabilistic models. Overall, there are many opportunities for further research and development in this area, and these are just a few examples of the ways in which the work presented in this paper could be extended and refined.

5. References

[1] Dhimish, M., Vieira, R. G., & Badran, G. (2021). Investigating the stability and degradation of hydrogen PEM fuel cell. *International Journal of Hydrogen Energy*, *46*(74), 37017-37028.

[2] Ahmadi, P., & Khoshnevisan, A. (2022). Dynamic simulation and lifecycle assessment of hydrogen fuel cell electric vehicles considering various hydrogen production methods. *International Journal of Hydrogen Energy*, *47*(62), 26758-26769.

[3] Dhimish, M., & Schofield, N. (2022). Single-switch boost-buck DC-DC converter for industrial fuel cell and photovoltaics applications. *International Journal of Hydrogen Energy*, *47*(2), 1241-1255.

[4] Zhao, M., Huang, T., Liu, C., Chen, M., Ji, S., Christopher, D. M., & Li, X. (2021). Leak localization using distributed sensors and machine learning for hydrogen releases from a fuel cell vehicle in a parking garage. *International Journal of Hydrogen Energy*, *46*(1), 1420-1433.

[5] Chen, H., Shan, W., Liao, H., He, Y., Zhang, T., Pei, P., ... & Chen, J. (2021). Online voltage consistency prediction of proton exchange membrane fuel cells using a machine learning method. *International Journal of Hydrogen Energy*, *46*(69), 34399-34412.

[6] Costamagna, P., De Giorgi, A., Moser, G., Serpico, S. B., & Trucco, A. (2019). Data-driven techniques for fault diagnosis in power generation plants based on solid oxide fuel cells. *Energy conversion and management*, *180*, 281-291.

[7] Li, W. Z., Yang, W. W., Wang, N., Jiao, Y. H., Yang, Y., & Qu, Z. G. (2020). Optimization of blocked channel design for a proton exchange membrane fuel cell by coupled genetic algorithm and three-dimensional CFD modeling. *International Journal of Hydrogen Energy*, *45*(35), 17759-17770.

[8] Yu, Z., Xia, L., Xu, G., Wang, C., & Wang, D. (2022). Improvement of the three-dimensional fine-mesh flow field of proton exchange membrane fuel cell (PEMFC) using CFD modeling, artificial neural network and genetic algorithm. *International Journal of Hydrogen Energy*, *47*(82), 35038-35054.

[9] Lee, Y., Park, E. T., Jeong, J., Shi, H., Kim, J., Kang, B. S., & Song, W. (2020). Weight optimization of hydrogen storage vessels for quadcopter UAV using genetic algorithm. *International Journal of Hydrogen Energy*, *45*(58), 33939-33947.

[10] Nasrabadi, A. M., & Moghimi, M. (2022). Energy analysis and optimization of a biosensor-based microfluidic microbial fuel cell using both genetic algorithm and neural network PSO. *International Journal of Hydrogen Energy*, *47*(7), 4854-4867.

[11] Fathy, A., Rezk, H., & Nassef, A. M. (2019). Robust hydrogen-consumption-minimization strategy based salp swarm algorithm for energy management of fuel cell/supercapacitor/batteries in highly fluctuated load condition. *Renewable energy*, *139*, 147-160.

[12] Nayak, P. C., Mishra, S., Prusty, R. C., & Panda, S. (2022). Performance analysis of hydrogen aqua equaliser fuel-cell on AGC of wind-hydro-thermal power systems with sunflower algorithm optimised fuzzy-PDFPI controller. *International Journal of Ambient Energy*, *43*(1), 3454-3467.

[13] Sulaiman, N., Hannan, M. A., Mohamed, A., Ker, P. J., Majlan, E. H., & Daud, W. W. (2018). Optimization of energy management system for fuel-cell hybrid electric vehicles: Issues and recommendations. *Applied energy*, *228*, 2061-2079.

[14] Chen, K., Laghrouche, S., & Djerdir, A. (2020). Aging prognosis model of proton exchange membrane fuel cell in different operating conditions. *International Journal of Hydrogen Energy*, *45*(20), 11761-11772.

[15] Yuan, H. B., Zou, W. J., Jung, S., & Kim, Y. B. (2022). Optimized rule-based energy management for a polymer electrolyte membrane fuel cell/battery hybrid power system using a genetic algorithm. *International Journal of Hydrogen Energy*, *47*(12), 7932-7948.

[16] Kishore, S. C., Perumal, S., Atchudan, R., Alagan, M., Sundramoorthy, A. K., & Lee, Y. R. (2022). A Critical Review on Artificial Intelligence for Fuel Cell Diagnosis. *Catalysts*, *12*(7), 743.

[17] Peksen, M. M. (2022). Artificial Intelligence-Based Machine Learning toward the Solution of Climate-Friendly Hydrogen Fuel Cell Electric Vehicles. *Vehicles*, *4*(3), 663-680.

[18] Zhao, J., Li, X., Shum, C., & McPhee, J. (2021). A Review of physics-based and data-driven models for real-time control of polymer electrolyte membrane fuel cells. *Energy and AI*, *6*, 100114.

[19] Leung, C. K., Braun, P., & Cuzzocrea, A. (2019). AI-based sensor information fusion for supporting deep supervised learning. *Sensors*, *19*(6), 1345.

[20] Rashidi, H. H., Tran, N., Albahra, S., & Dang, L. T. (2021). Machine learning in health care and laboratory medicine: General overview of supervised learning and Auto-ML. *International Journal of Laboratory Hematology*, *43*, 15-22.

[21] Han, Z., Li, J., Zhang, B., Hossain, M. M., & Xu, C. (2021). Prediction of combustion state through a semi-supervised learning model and flame imaging. *Fuel*, *289*, 119745.

[22] Venkatasatish, R., & Dhanamjayulu, C. (2022). Reinforcement learning based energy management systems and hydrogen refuelling stations for fuel cell electric vehicles: An overview. *International Journal of Hydrogen Energy*.

[23] Li, J., & Yu, T. (2021). A novel data-driven controller for solid oxide fuel cell via deep reinforcement learning. *Journal of Cleaner Production*, *321*, 128929.

[24] Gu, P., Xing, L., Wang, Y., Feng, J., & Peng, X. (2021). A multi-objective parametric study of the claw hydrogen pump for fuel cell vehicles using taguchi method and ANN. *International Journal of Hydrogen Energy*, *46*(9), 6680-6692.

[25] Szabłowski, Ł., Milewski, J., Badyda, K., & Kupecki, J. (2018). ANN–supported control strategy for a solid oxide fuel cell working on demand for a public utility building. *International Journal of Hydrogen Energy*, *43*(6), 3555-3565.

[26] Vieira, R. G., Dhimish, M., de Araújo, F. M., & Guerra, M. I. (2020). PV module fault detection using combined artificial neural network and sugeno fuzzy logic. *Electronics*, *9*(12), 2150.

[27] Gallo, M., Costabile, C., Sorrentino, M., Polverino, P., & Pianese, C. (2020). Development and application of a comprehensive model-based methodology for fault mitigation of fuel cell powered systems. *Applied Energy*, *279*, 115698.

[28] Ritzberger, D., Höflinger, J., Du, Z. P., Hametner, C., & Jakubek, S. (2021). Data-driven parameterization of polymer electrolyte membrane fuel cell models via simultaneous local linear structured state space identification. *International Journal of Hydrogen Energy*, *46*(21), 11878-11893.

[29] Gu, X., Hou, Z., & Cai, J. (2021). Data-based flooding fault diagnosis of proton exchange membrane fuel cell systems using LSTM networks. *Energy and AI*, *4*, 100056.

[30] Zhou, S., Lu, Y., Bao, D., Wang, K., Shan, J., & Hou, Z. (2022). Real-time data-driven fault diagnosis of proton exchange membrane fuel cell system based on binary encoding convolutional neural network. *International Journal of Hydrogen Energy*, *47*(20), 10976-10989.

[31] Xing, Y., Wang, B., Gong, Z., Hou, Z., Xi, F., Mou, G., ... & Jiao, K. (2022). Data-driven Fault Diagnosis for PEM Fuel Cell System Using Sensor Pre-Selection Method and Artificial Neural Network Model. *IEEE Transactions on Energy Conversion*.